Supplementary Information

Human Corneal Expression of SLC4A11, a Gene Mutated in Endothelial Corneal Dystrophies

Darpan Malhotra[1], Sampath K. Loganathan[1,2], Anthony M. Chiu[1], Chris M. Lukowski[1] and Joseph R. Casey[1#]

[1]Department of Biochemistry, Membrane Protein Disease Research Group, University of Alberta, Edmonton, Alberta, T6G 2H7, Canada.

[2]Present address: Lunenfeld-Tanenbaum Research Institute, Toronto, Ontario, Canada M5G 1X5

[#]Address Correspondence to:
Dr. Joseph R. Casey
Department of Biochemistry
University of Alberta
Edmonton, Alberta, Canada T6G 2H7
Phone: (780) 492-7203
Email: joe.casey@ualberta.ca
URL: http://www2.biochem.ualberta.ca/CaseyLab/index.php

SUPPLEMENTARY FIGURE LEGENDS

Supplementary Figure S1. Detection ratio of SLC4A11-common antibody vs. SLC4A11-v3 antibody for SLC4A11 v3 protein. HEK293 cells transfected with cDNA encoding SLC4A11 v3 were processed for immunoblots. 5 µg, 10 µg and 20 µg of cell lysate was loaded in duplicates. Blots were probed with SLC4A11-common antibody (α-common) and SLC4A11-v3 (α-v3) antibody. Densitometry quantified the band intensities. Ratio of SLC4A11 band intensity from α−common and α−v3 antibodies was calculated for each amount of total lysate and plotted. Data represent mean ± SEM from three replicates.

Supplementary Figure S2. Alternative homology model of SLC4A11 v2-M36 and SLC4A11 v3 cytoplasmic domains. Homology models of cytoplasmic domains of (**A**) SLC4A11 v2-M36 and (**B**) SLC4A11 v3 generated by Phyre2 fold recognition software, using crystal structure of human erythrocyte Band 3 cytoplasmic domain (PDB: 1HYN) as the template. Unique N-terminal sequence of v3 is highlighted in pink. (**C**) v2-M36 and v3 models aligned in PyMOL (molecular graphics system version 2.0.7), using segments that were modelled with 100% confidence (R90-P306 for v2-M36, R109-P325 for v3). N_{v2}, N_{v3} and C_{v2}, C_{v3} are the N and C termini for v2-M36 and v3, respectively.

Supplementary Figure S3. Full-length immunoblot images for the data presented in Figure 3. Blots 1 and 2 were probed with α-SLC4A11-common and α-SLC4A11-v3 antibodies, respectively. Blots probed with α-GAPDH antibody are presented below their

respective samples. Intervening lanes to the left of human cornea lane are shown. MW: Molecular weight.

Supplementary Figure S4. Full-length immunoblot images for the data presented in Figure 5A.

Supplementary Figure S5. Full-length immunoblot images for the data presented in Figure 6A.
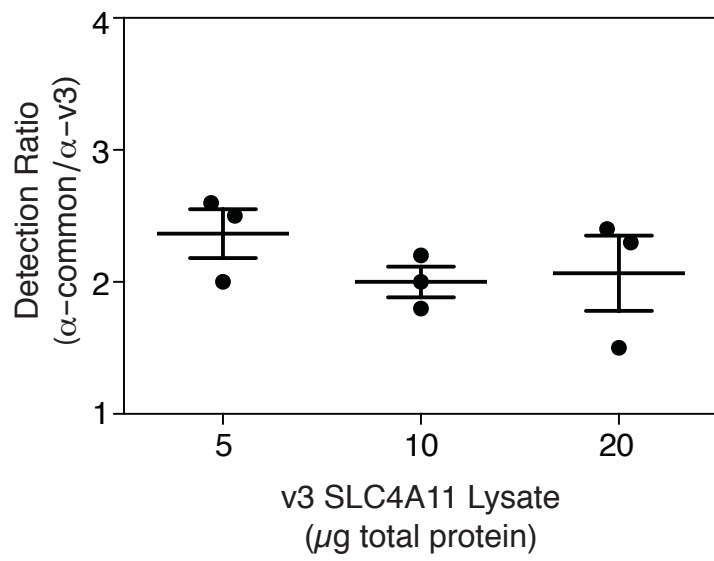
SUPPLEMENTARY TABLES

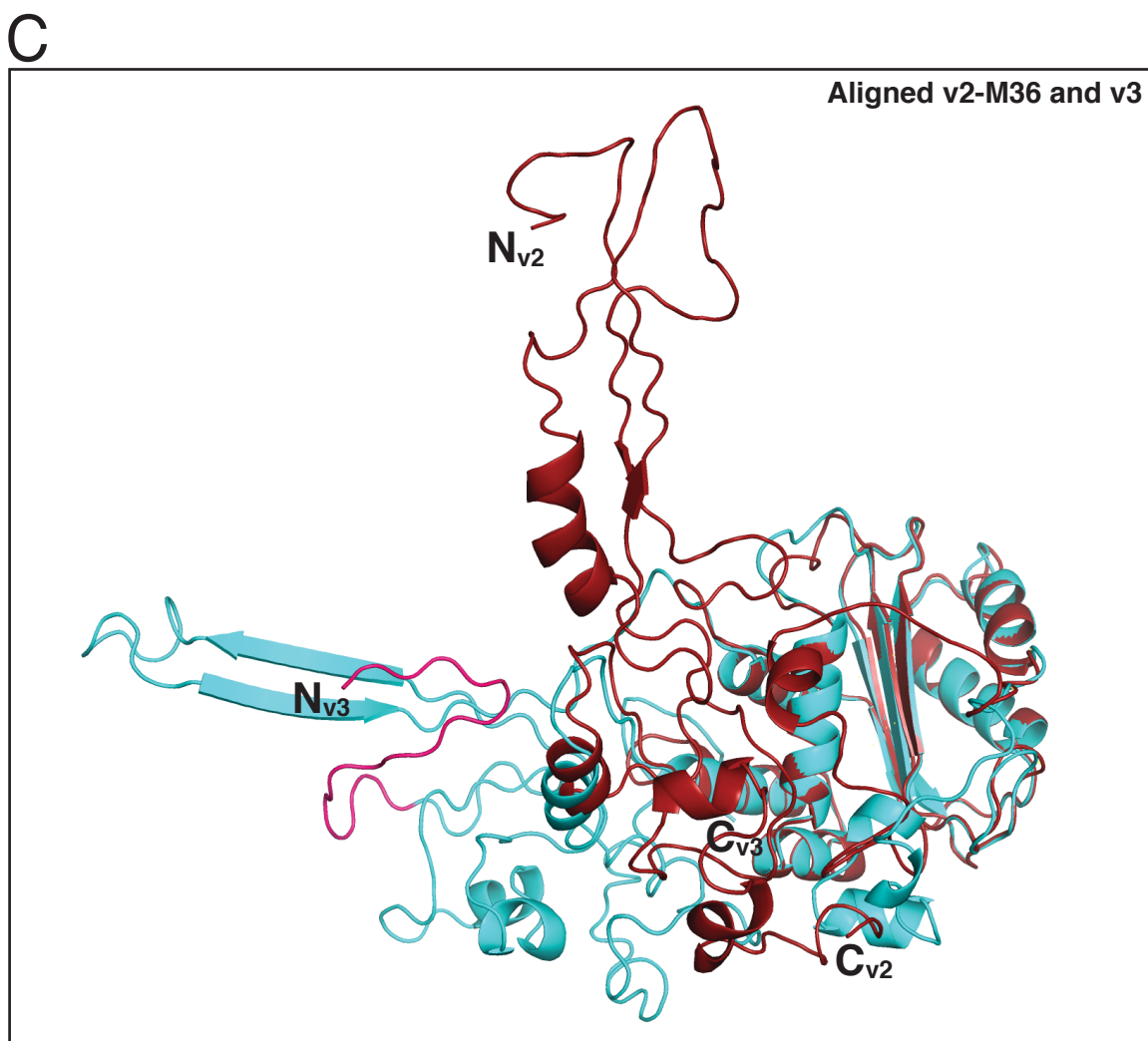**Supplementary Table S1. Primers for reverse transcription PCR amplification of SLC4A11 transcripts.**
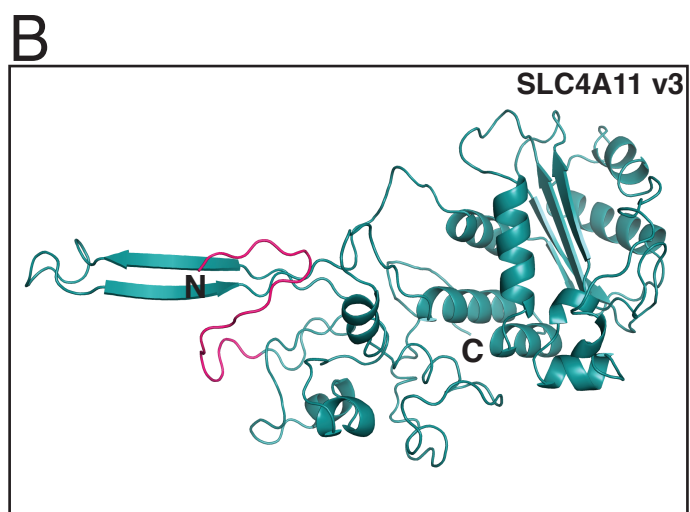
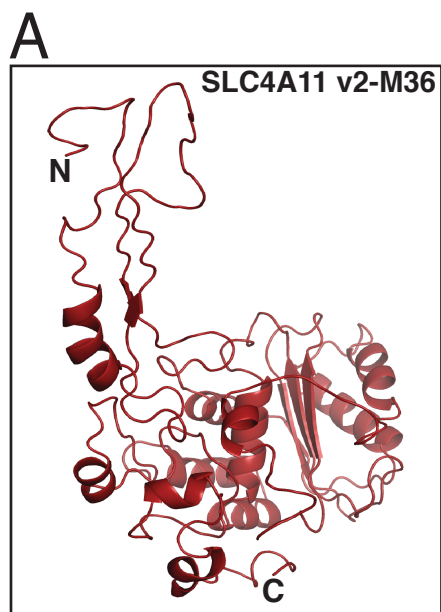|	Forward Primer	Reverse Primer	Product Size (bp)
SLC4A11 Variant 1	5'-GGGCAGGGTTTTCTCAGGAA-3'	5'-CATTCTCAGTGTTGGTGGCCT-3'	244
SLC4A11 Variant 2	5'-GGCTGGTGACCTTTCTGCTT-3'	5'-CATTCTCAGTGTTGGTGGCCT-3'	233
SLC4A11 Variant 3	5'-CAGGCGCGTGTTCCATCTG-3'	5'-CATTCTCAGTGTTGGTGGCCT-3'	233
GAPDH	5'-CAGCCTCAAGATCATCAGCA-3'	5'-TGTGGTCATGAGTCCTTCCA-3'	106

Supplementary Table S2. Review of Human SLC4A11 Variants used in studies from 2001-2019. Studies using different SLC4A11 variants since 2001. Indicated citations can be found in the main references.
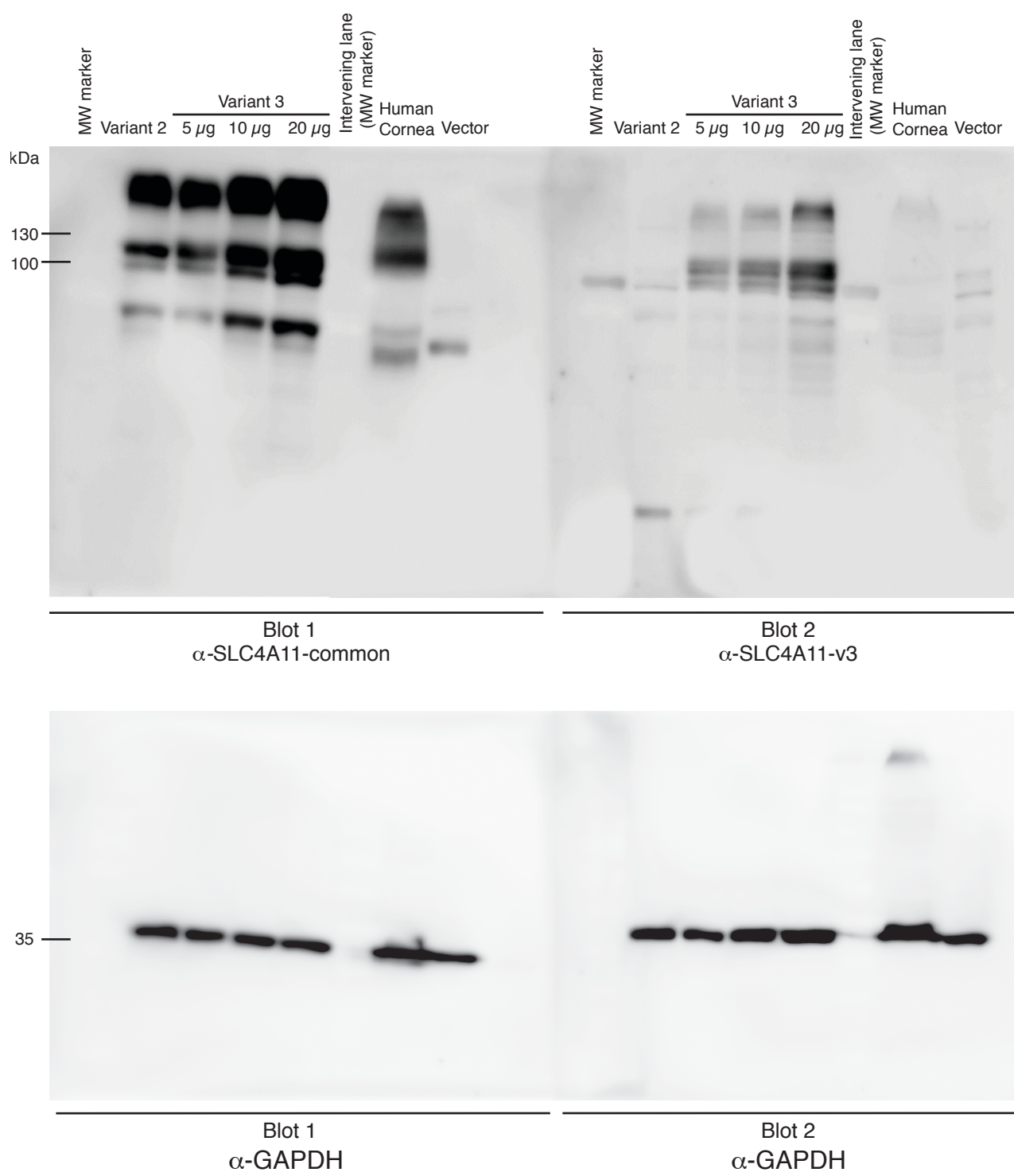
SLC4A11 Variant used	Literature Citations with Reference Numbers in Manuscript
v1	Zhang *et al.* (2015)[20]
v2-M1	Parker *et al.* (2001)[44], Park *et al.* (2004)[23], Vithana *et al.* (2006)[10], Riazuddin *et al.* (2010)[5], Vilas *et al.* (2011)[29], Vilas *et al.* (2012)[28], Jalimarada *et al.* (2013)[16], Vilas *et al.* (2013)[14], Ogando *et al.* (2013)[17], Loganathan *et al.* (2014)[15], Soumittra *et al.* (2014)[27], Roy *et al.* (2015)[45], Loganathan *et al.* (2016)[26], Kao *et al.* (2016)[46], Guha *et al.* (2017)[47], Li *et al.* (2019)[25]
v2-M36	Chiu *et al.* (2016)[48], Loganathan *et al.* (2016)[21], Badior *et al.* (2017)[49], Alka *et al.* (2018a)[24], Alka *et al.* (2018b)[50]
v3	Kao *et al.* (2015)[18], Kao *et al.* (2016)[46]

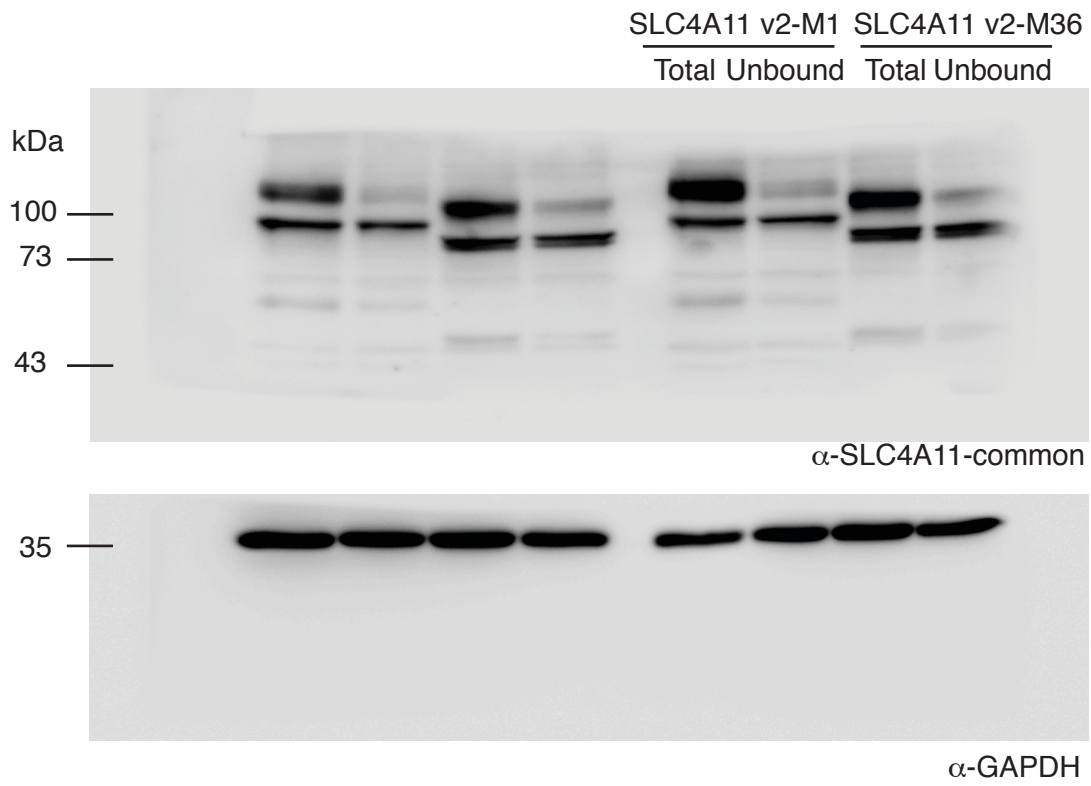Supplementary Figure S1

A SLC4A11 v2-M36
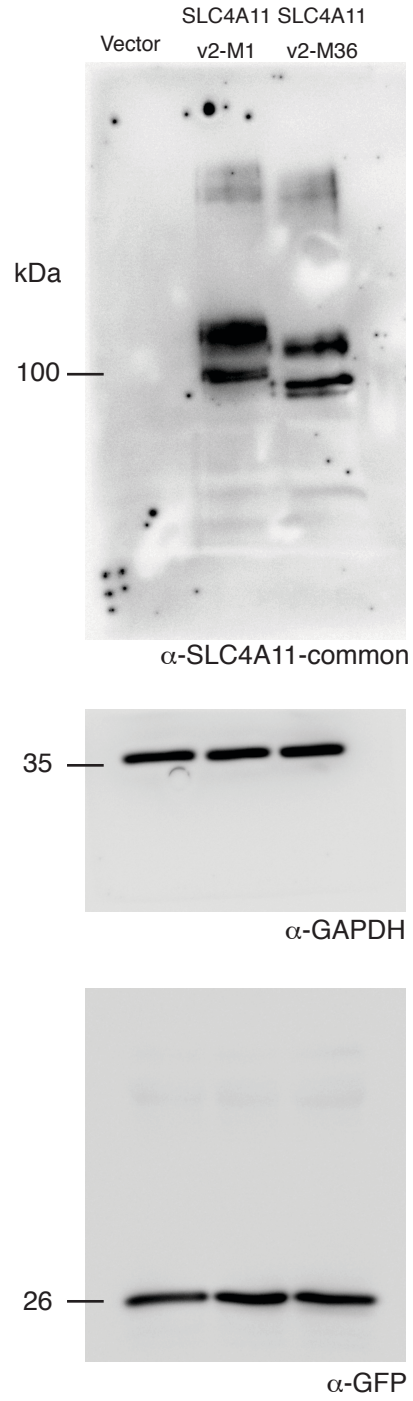
B SLC4A11 v3

C Aligned v2-M36 and v3

Supplementary Figure S2

Supplementary Figure S3

Supplementary Figure S4

Supplementary Figure S5